QED TESTS: UPPER LIMITS ON CUTOFF PARAMETERS AND ELECTROWEAK EFFECTS*

By G. Knies

DESY, Hamburg**

(Received October 22, 1981)

Tests of Quantum Electrodynamics by the reactions $e^+e^- \to e^+e^-$, $\mu^+\mu^-$, $\tau^+\tau^-$ and $\gamma\gamma$ at center of mass energies of up to 31 GeV are described. The measurements were done at the e^+e^- storage ring PETRA at DESY in Hamburg mainly with the PLUTO detector. Results on QED cutoff parameters Λ, and an electroweak effects are given.

PACS numbers: 12.20.Fv

1. Introduction

Quantum electrodynamics (QED) is known to describe a vast amount of electromagnetic phenomena to a high precision. It has evolved from an understanding of macroscopic electromagnetic phenomena, in terms of charges and electromagnetic fields, leading to Maxwell's equations. Field quantization together with the Dirac equation for fermions then yielded QED which allows for prediction of the interaction of photons with particles having pointlike charges, also at microscopic distances — or large momentum transfers — including the creation of particle-antiparticle pairs. Since the early days of QED it has therefore been of great interest [1] to find out whether below some very short distances — or beyond some very large momentum transfers — nature is different from the picture QED is based on. The high energies of PETRA allowed for a further step in testing the validity of QED, namely up to momentum transfers of ~ 1000 GeV^2, or down to distances of $< 10^{-15}$ cm.

Deviations from pure QED are expected:

(*i*) from the hadronic vacuum polarization [2],

(*ii*) from weak neutral current interactions [3],

(*iii*) as a general breakdown at large space like ($q^2 < 0$) or time like ($q^2 = s > 0$) momentum transfers, or short distances, e.g. as a consequence of a non pointlike nature of the charges involved or from excited heavy states of the leptons [4].

---

* Presented at the XX Cracow School of Theoretical Physics, Zakopane, May 29 — June 11, 1980.

** Address: DESY, Notkestr. 85, D-2000 Hamburg 52, West Germany.

In e^+e^- storage ring experiments such deviations from QED can be looked for in the following reactions:

$$e^+e^- \to e^+e^- \quad (1)$$

$$\mu^+\mu^- \quad (2)$$

$$\tau^+\tau^- \quad (3)$$

$$\gamma\gamma \quad (4)$$

and in final states containing additional photons or lepton pairs. The hadronic vacuum polarization has been most clearly observed, and measured quantitatively as a sizeable effect in reactions (1) and (2) at the energies of the ϱ, ω, ϕ, J/ψ and T resonances [5], and will not be pursued further here. As a "trivial" modification of QED it is included in the radiative corrections (see below). No other deviations from pure QED have been observed so far in these reactions[1] [1]. But since relative deviations due to (*ii*) and (*iii*) are expected to grow like s or even faster, experiments at PETRA are 10 times more sensitive than the best previous tests [8]. In processes with time like photon propagators, interference with the weak neutral current grows proportional to s and produces deviations from pure QED cross sections of up to a few percent at $s \approx 1000\ \text{GeV}^2$. These effects show up in the reactions (1)–(3). Effects from other modifications (*iii*), parameterized by so called QED cutoff parameters Λ, can also be studied in reactions (1)–(3), and in addition in reaction (4). This latter reaction has no first order weak interaction contribution.

In the following subsection we describe the nomenclature of writing QED cross sections, and of incorporating modifications. Then we present the corresponding exeprimental results. Their implications for the QED cutoff parameters, and for electroweak effects are discussed in Sections 4, and 5, respectively. In Appendix A we give a compilation of formulae used to describe these deviations. Finally, in Appendix B we include an account of the data analysis of the four QED reactions.

2. Radiative corrections and QED modifications

For a comparison of QED predictions with the data of reactions (1)–(4), the theoretical predictions are usually given in terms of first order QED cross sections, σ_1^{QED} (see diagrams in Figs 1 and 2) and, to account for effects from higher order QED diagrams and from hadronic vacuum polarization (Figs 3 and 4), by the so called radiative corrections δ_{RAD}:

$$\sigma^{\text{QED}} = \sigma_1^{\text{QED}}(1+\delta_{\text{RAD}}). \quad (5)$$

On the r.h.s. σ_1^{QED} is a purely theoretical quantity whereas the radiative corrections depend on the detector resolution and on acceptance cuts for events in reactions (1)–(4). Therefore one usually corrects (using QED) the experimental cross section σ^{EXP}, which is already

[1] Electroweak interference effects have been measured with high precision in polarized electron nucleon scattering at SLAC at low momentum transfers [6], and also in optical rotation of linearly polarized laser light at Novosibirsk [7].

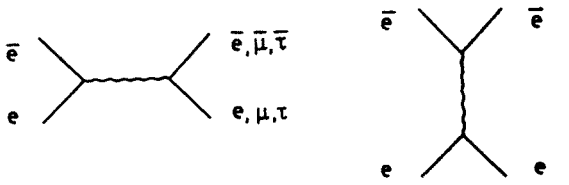

Fig. 1. First order QED diagrams for $e^+e^- \to l^+l^-$

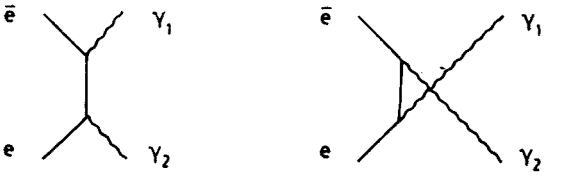

Fig. 2. First order QED diagrams for $e^+e^- \to \gamma\gamma$

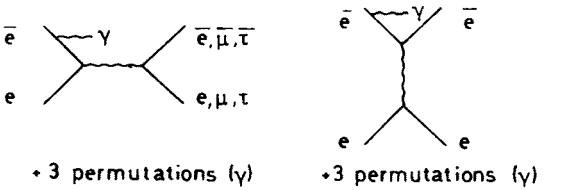

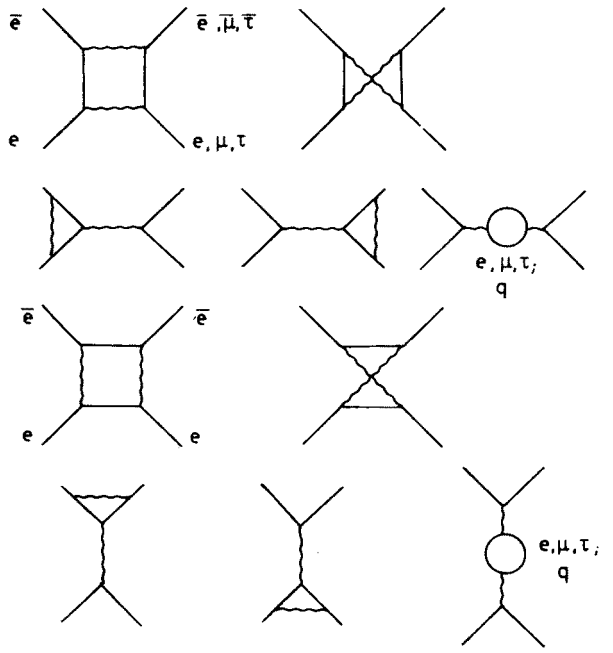

Fig. 3. Diagrams contributing to radiative corrections of order α^3, for $e^+e^- \to l^+l^-$

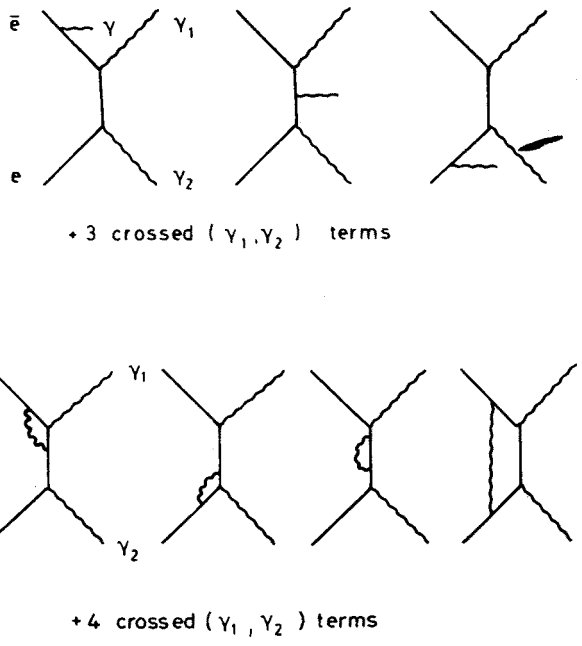

Fig. 4. Diagrams contributing to radiative corrections of order α^3, for $e^+e^- \to \gamma\gamma$

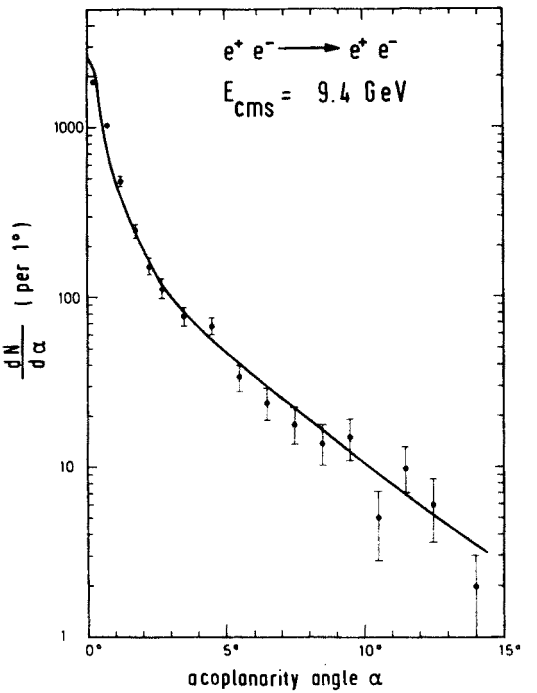

Fig. 5. Distribution of the acoplanarity angle α from the Bhabha event sample, at $W = 9.4$ GeV

corrected for acceptance, with δ_{RAD} such that it can be compared directly to σ_1^{QED} (if $\delta_{RAD} \ll 1$):

$$\sigma^{CORR} = \sigma^{EXP}(1-\delta_{RAD}). \tag{6}$$

The radiative and the hadronic vacuum polarization corrections δ_{RAD} have been calculated up to order α^3 by Refs [9, 10] (see diagrams in Figs 3 and 4). Since the deviations we are looking for are of similar size as the calculated radiative corrections it is important to check the radiative corrections independently. This is possible in radiative Bhabha scatters with hard photons (i.e. $e^+e^- \to e^+e^-\gamma$) which are partly accepted by the criteria for the Bhabha sample. Because of the — unobserved or unresolved — photon, the final state e^+ and e^- particles are in general no longer coplanar with the beams. In Fig. 5 we show the predicted acoplanarity angle distribution. It has a large angle tail from hard photon radiation, mainly in the initial state, and agrees very well with the observed acoplanarity distribution. The width of the peak at small angles reflects the angular resolution.

The QED predictions also depend on beam polarization. All cross section predictions given here are assuming no beam polarization. A transverse beam polarization which is expected for e^+e^- storage rings [24] does not affect the analysis described here since we have a uniform acceptance in the azimuthal angle. No longitudinal polarization is expected since there are no horizontal fields strong enough to rotate a possible transverse polarization.

The first order predictions of modified versions of QED can be written in terms of first order pure QED predictions as

$$\sigma_1^{MOD} \equiv \sigma_1^{QED}(1+\delta_\Lambda+\delta_w), \tag{7}$$

with δ_Λ for general large q^2 QED breakdown effects and δ_w for electroweak interference effects.

If we assume that radiative corrections for σ_1^{MOD} are similar to those for σ_1^{QED} we can determine δ_Λ and δ_w from the data through

$$\sigma^{CORR} = \sigma^{QED}(1+\delta_\Lambda+\sigma_w). \tag{8}$$

Since later we find $\sigma^{CORR} = \sigma_1^{QED}$ within the accuracy of the data, we determine limits on possible modifications, by setting $\delta_w = 0$ for limits on δ_Λ, and vice versa.

Explicit expressions for δ_Λ and δ_w can be given in specific models, and limits on δ_Λ and δ_w can then be translated into limits on parameters of these models. In Appendix A we summarize expressions for these QED modifications.

The electroweak deviations δ_w are calculated by adding Z^0 exchange diagrams to the one photon exchange diagrams in Fig. 1. The electroweak effects then depend on 3 free parameters: v^2, a^2 and M_Z, which are related to the electroweak ("Salam-Weinberg") mixing angle θ_w in the GSW theory [3]. The total cross section modifications depend mainly on the vector current coupling v^2, while the μ pair charge asymmetry [11] depends mainly on the axial current coupling a^2. The mass M_Z affects the energy dependence of electroweak effects.

The deviations δ_Λ from breakdowns of QED at large momentum transfers are expressed as modifications of lepton-photon vertex functions or propagators [4]. In the first order amplitudes for ee → ee, μμ and ττ the two lepton-photon-lepton vertices and the photon propagator are multiplied by momentum transfer dependent factors $V(q^2)$ (for the vertex) and $D(q^2)$ (for the propagator). They can be combined into one overall form factor F for the scattering amplitude:

$$V_T^2(s) \cdot D_T(s) = F_T(s) \quad \text{for the time like amplitude,} \tag{9a}$$

$$V_S^2(q^2) \cdot D_S(q^2) = F_S(q^2) \quad \text{for the space like amplitude.} \tag{9b}$$

The modifications can be different at space like and at time like momentum transfers, and also different for the e, μ and τ leptons. Since no deviations from QED are observed in any of the four reactions (1)–(4) we assume (*i*) electromagnetic lepton universality, i.e. the same vertex function for different leptons, and (*ii*) the same form factor parameterizations for time like and space like momentum transfers, and (*iii*) we consider only the lowest possible orders in q^2 for the form factors.

For the lepton pair channels (reactions (1)–(3)) we use the form factor parametrization

$$F(q^2) = 1 \pm \frac{q^2}{\Lambda_\pm^2}, \tag{10}$$

which can be considered the first order approximation in q^2/Λ^2 for the formfactor $F = \Lambda_\pm^2/(\Lambda_\pm^2 \mp q^2)$ proposed in the literature [4]. Two cutoff parameters, Λ_+ and Λ_-, are introduced to allow for $F \geqslant 1$ nad $F \leqslant 1$. $\Lambda = \infty$ restores pure QED. Λ_+ can be related in the static limit to the charge radius of leptons. If e and γ are pointlike particles, but μ or τ leptons were independently extended we would measure their charge radius in reactions (2) and (3) as [1]

$$\langle r^2 \rangle = \frac{6\hbar^2 c^2}{\Lambda_+^2} = \frac{3\hbar^2 c^2}{s}\left(\frac{\sigma^{\text{CORR}}}{\sigma_1^{\text{QED}}} - 1\right). \tag{11}$$

Finite values of Λ_- can arise from a heavy neutral particle interfering with the photon in reactions (1)–(3).

In the γ pair channel (reaction (4)) the QED violations as discussed for the lepton pair channels cannot produce deviations proportional to Q^2 because of cancellations due to current conservation [4e, 4g, 12]. In this case, the so called "sea gull" graph [4g, i] gives rise to a q^4/Λ^4 term in the form factor:

$$F(q^2) = 1 \pm q^4/\Lambda_\pm^4. \tag{12}$$

A slightly different cross section modification for ee → γγ arises from the exchange of a virtual excited (heavy) electron [4h].

To illustrate the effect of the modifications, we show in Figs 6 c-f how the modified QED predictions for reactions (1)–(3) depend on different values of the cutoff parameters $\Lambda_\pm$, and of the Salam-Weinberg angle θ_w. In Bhabha scattering the cross sections at small

angles (mainly space like contributions, small $|q^2|$) are almost unaffected. Only the large angle part is sensitive. Both modifications have much stronger effects (by a factor ~ 3) in lepton pair production, than in Bhabha scattering, since there all contributions come

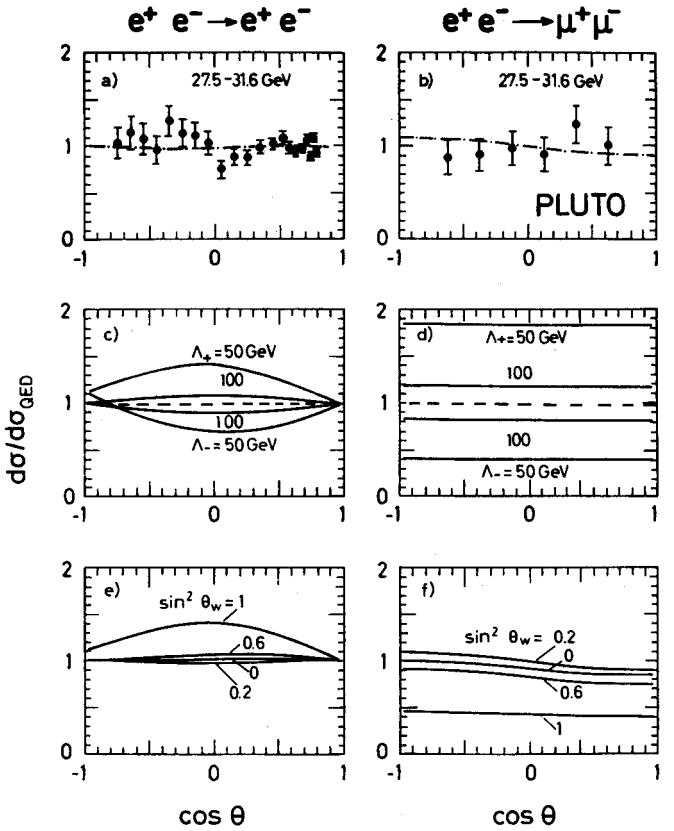

Fig. 6. Differential cross section $d\sigma^{CORR}/d\sigma_1^{QED}$ for (a) $e^+e^- \to e^+e^-$ and (b) $e^+e^- \to \mu^+\mu^-$; $d\sigma_1^{MOD}/d\sigma_1^{QED}$ for QED modifications by form factors (c, d) and by electroweak interference (e, f)

from the time like diagram with a high value of $q^2 = s^2$. The forward/backward (or: charge) asymmetry A in the lepton pair production reactions (2) and (3):

$$A = \frac{\sigma(\cos\theta > 0) - \sigma(\cos\theta < 0)}{\sigma(\cos\theta > 0) + \sigma(\cos\theta < 0)} \tag{13}$$

is still rather small at $s \approx 1000\ \mathrm{GeV}^2$ ($\sim -6\%$) if $M_Z \gtrsim 90$ GeV, and requires a high statistics measurement.

In photon pair production (4) the high q^2 QED modifications affect the size and the

[2] The better statistical accuracy in the e^+e^- channel leads however to a similar sensitivity for QED violations in reaction (1).

shape of differential cross sections. Since deviations here are proportional to q^4/Λ^4 the expected cross section modifications are much smaller than in lepton pair production, at comparable values of Λ.

3. *The data*

Reactions (1)–(4) have been measured with PLUTO [13] and also in other PETRA experiments [14]. In Table I we summarize the event numbers observed in the PLUTO experiment, and the acceptance cuts in the four channels. Further details on the data analysis are given in Appendix B.

TABLE I

Acceptance cuts and event numbers in the QED reactions

Reaction $e^+e^- \to$	# of events	Production angle $\lvert\cos\theta\rvert <$	Acollinearity angle $\alpha <$
e^+e^-	5700	0.8	15°
$\mu^+\mu^-$	228	0.75	10°
$\tau^+\tau^-$	139	—[a]	—
$\gamma\gamma$	1020	0.75	20°

[a] In 2 prongs $\lvert\cos\theta\rvert < 0.6$ for each track, and in 4 prongs $\lvert\cos\theta\rvert < 0.75$ for each track.

The luminosities needed for calculating cross sections are determined from Bhabha scattering at small forward angles ($0.7 < \cos\theta < 0.8$) where $|q^2|$ is much smaller than s($|q^2| \approx 0.1s$). Therefore the effect of any QED modification on luminosity determination is negligible as compared to its effect on the lepton pair production cross section at $q^2 = s$, as can be seen in Fig. 6 c-f.

The total cross sections for μ, τ and γ pair production are shown in Figs 7a, b and c, as a function of s. They show the expected $1/s$ dependence and agree with the QED cross section. In Figs 6 a and b we show the ratio $d\sigma^{\mathrm{CORR}}/d\sigma_1^{\mathrm{QED}}$ versus $\cos\theta$ for ee and $\mu\mu$, averaged over data of $27.5 < W < 31.6$ GeV. At all data points this ratio is consistent with 1. The ratio is trivially equal to 1 for forward Bhabha scattering ($0.7 < \cos\theta < 0.8$) which has been used to determine the luminosity[3]. The μ pair asymmetry, derived from Fig. 6b (for $|\cos\theta| < 0.75$, $s = 911$ GeV^2) is

$$A = 7\% \pm 8\% \text{ (stat.)} \pm 2\% \text{ (syst.)} \tag{14}$$

compared to -5.8% expected in the standard electroweak model [3] for $\sin^2\theta_w = 0.23$. Finally the differential cross section for ee $\to \gamma\gamma$ is shown in Fig. 8. In the latter figure the data is not corrected for δ_{RAD} and resolution. These effects are included here in the theoretical curves.

[3] Actually we used the electroweak cross section σ^{EW} for Bhabha scattering with $\sin^2\theta_w = 0.23$ (see App. A) instead of σ^{QED} to determine the luminosity. The difference is $< 1\%$ at these angles.

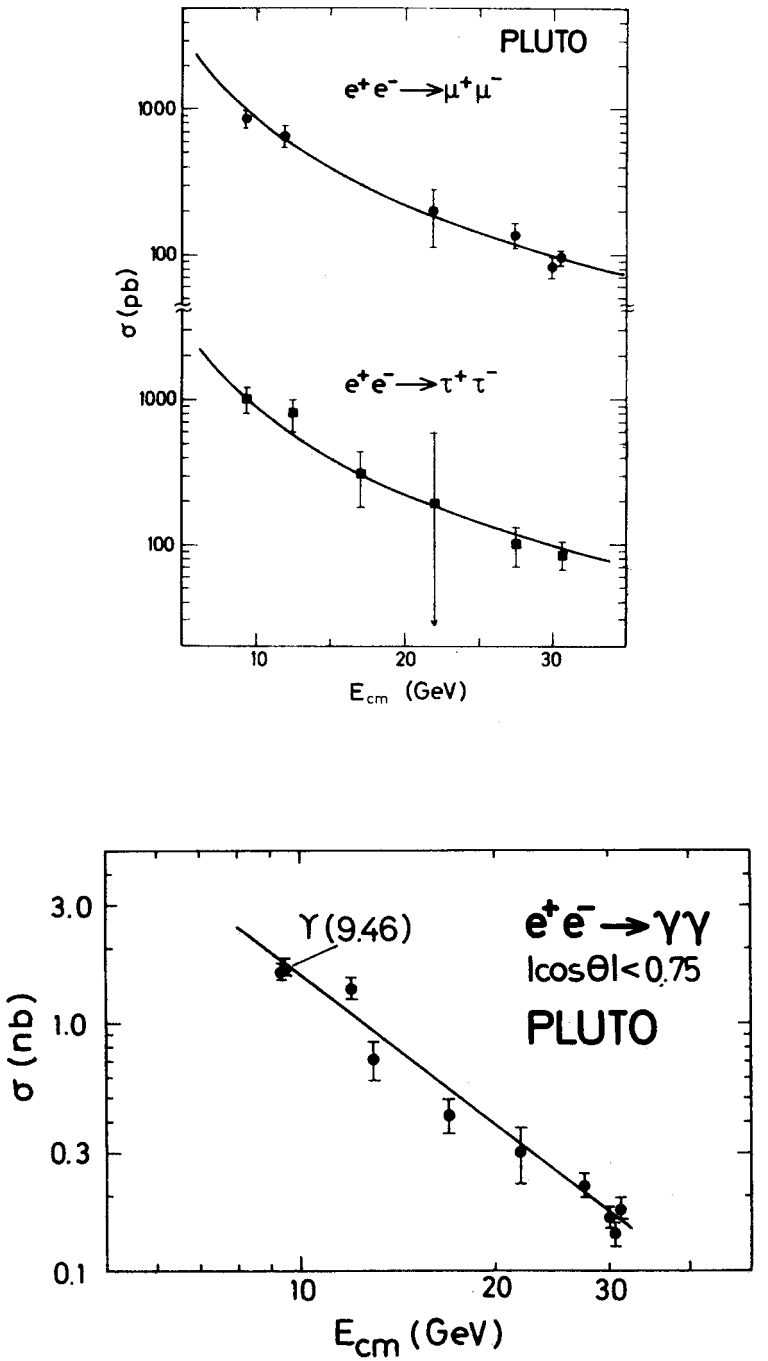

Fig. 7. Total cross section σ^{CORR} for the reactions (a) $e^+e^- \to \mu^+\mu^-$ and $\tau^+\tau^-$, and (b) for $e^+e^- \to \gamma\gamma$ at $|\cos\theta| < 0.75$ as function of energy, after corrections for acceptance and radiative processes (see Eq. (6)). Curves are first order QED cross sections

There is no evidence in any of the distributions for a deviation from pure QED. This null result — together with the errors — will be expressed in the two following sections in terms of limits on parameters describing possible deviations.

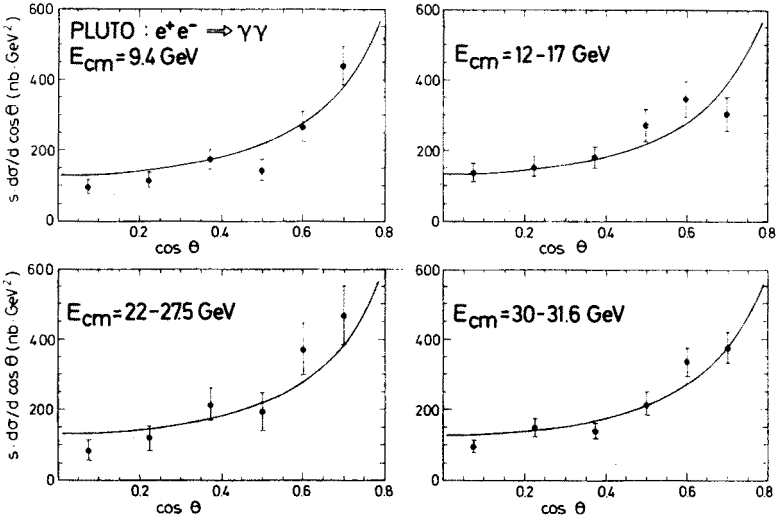

Fig. 8. Differential cross section $sd\sigma/d\cos\theta$ for $e^+e^- \to \gamma\gamma$, at 4 energies, not corrected for radiative effects and angular resolution. The curves are the corresponding QED prediction, with radiative corrections up to order α^3

4. QED cutoff parameters

From the data shown in the previous section we can infer limits on the cutoff parameters Λ in the form factors (Eqs (10) and (12)). The limits given in Table II have been determined separately from each of the reactions (1)–(4) with the assumptions discussed in Section 2.

TABLE II

Lower limits (95% c.l.) on QED cutoff parameters Λ, in GeV, as determined in the reactions (1) - (4). Cases $\gamma\gamma$ (a) and $\gamma\gamma$ (b) are explained in the text

	ee	$\mu\mu$	$\tau\tau$	$\gamma\gamma$(a)	$\gamma\gamma$(b)
Λ_+	234	107	79	46	46
Λ_-	80	101	63	36	—

More detailed cutoff parameters Λ can be introduced in the lepton pair channels by dropping the assumption of electromagnetic lepton universality and by allowing for independent space like and time like cutoff parameters, Λ_S and Λ_T, in Eq. (10). Results along these lines are given in Ref. [13a].

The limits on Λ (Table II) from the $\gamma\gamma$ channel are weaker since the form factor here depends on $(1/\Lambda)^4$ rather than $(1/\Lambda)^2$. In column $\gamma\gamma$ (a) Λ is the QED cutoff parameter of the form factor (12) which multiplies the first order amplitudes for reactions (4). In column $\gamma\gamma$ (b) the parameter Λ_+ is related to the mass of an exchanged (hypothetic) excited electron. Here the limit for Λ_+ can be interpreted as a lower mass limit for the excited electron, if it has a magnetic coupling to the electron with a "natural" strength [4h]. There is no physical motivation for a corresponding Λ_- parameter.

5. Electroweak effects

Assuming that there are no other modifications of QED ($\delta_\Lambda = 0$) we can use the combined data in Fig. 6a, b from reactions (1)–(2) to place limits on the electroweak parameters.[4] First we evaluate for a single neutral boson model the limits on the vector and the axial current couplings, v^2 and a^2, and on M_Z as independent quantities. Then we link these parameters through the Salam-Weinberg angle θ_w and determine an upper limit on $\sin^2\theta_w$. Finally we infer limits on boson masses for models with 2 neutral gauge bosons. For definitions and formulae we refer to Appendix A.

5.1. Limits on v^2, a^2 and M_Z

As a first step we set $M_Z = \infty$ which gives the weakest constraints on v^2 and a^2 in a fit to our data:

$$v^2 = -0.09 \pm 0.60 \pm 0.29, \tag{15a}$$

$$a^2 = -0.77 \pm 0.96 \pm 0.09. \tag{15b}$$

These numbers are consistent with $v^2 = a^2 = 0$, i.e. with the absence of any weak interaction effects, but also with the standard electroweak model [3]:

$$a^2 = 1, \quad v^2 = 0.0064 \text{ for } \sin^2\theta_w = 0.23.$$

The results on v^2 and a^2 (4.15) are correlated (see App. A, Eqs (A.5) and (A.6)). Fig. 9 shows the 95% c.l. contour from the ee and $\mu\mu$ data in the a^2, v^2 plane, both for $M_Z = \infty$ and for $M_Z = 80$, 60, 40 GeV. In combination with the 2 (ambiguous) results for a^2 and v^2 from elastic νe scattering data [15] we can exclude Z^0 masses < 40 GeV. Furthermore, our data slightly favour the νe solution with small v^2 and dominating a^2.

The lower limits for Λ_- (Table II) cannot be trivially converted into a limit on M_Z. Although the electroweak and the cutoff parametrization have (first order) poles at $s = M_Z^2$ and $s = \Lambda_-^2$, respectively, their functional dependences on s/M_Z^2 and s/Λ_-^2, respectively, are different.

---

[4] Rection (3) — which in principle carries also the information provided by reaction (2) — is not used in this analysis since (*i*) the detection efficiency is only ~20%, and (*ii*) the production angle of τ pairs is not measured.

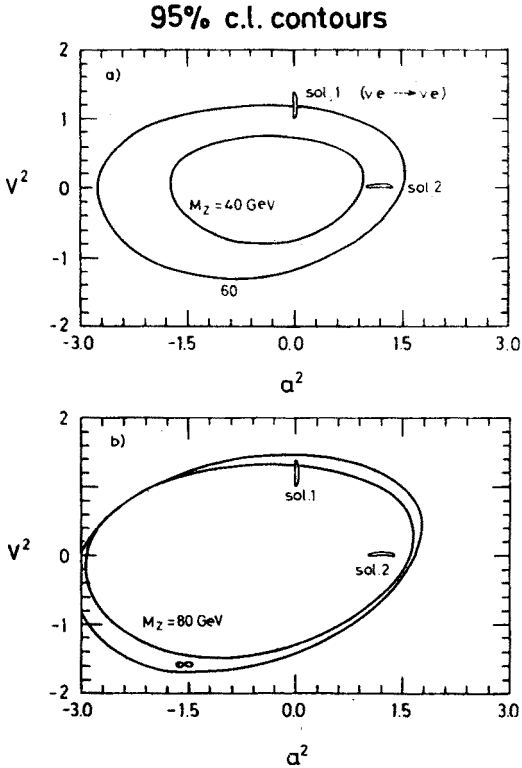

Fig. 9. 95% c.l. contour plots from fits of v^2 and a^2 to the data of Fig. 7a,b (a)assuming Z^0 masses of 40 and 60 GeV, (b) assuming Z^0 masses of 80 and ∞ GeV. Also shown are the two solutions for v^2 and a^2 as derived from elastic neutrino electron scattering [15]

5.2. Limits on the Salam-Weinberg angle θ_w

In the standard electroweak model [3] $\sin^2\theta_w$ is the only parameter, and we have the relations

$$a^2 = 1, \quad v^2 = (1-4\sin^2\theta_w)^2, \tag{16a, b}$$

$$M_Z^2 = \left(\frac{37.4\ \text{GeV}}{\sin\theta_w \cos\theta_w}\right)^2. \tag{16c}$$

With these constraints a fit to our data yields

$$\sin^2\theta_w = 0.22 \pm 0.22, \tag{17a}$$

or

$$\sin^2\theta_w < 0.52 \text{ at } 95\% \text{ c.l.} \tag{17b}$$

The result is consistent with the world average of $\sin^2\theta_w = 0.228 \pm 0.010$ [16], obtained from $\gamma - Z_0$ interference at much lower momentum transfers.

5.3. Models with 2 neutral gauge bosons

There are extensions of the standard model by a further symmetry group G to $SU_L(2) \times U(1) \times G$ in such a way that the predictions of the $SU_L(2) \times U(1)$ model are reproduced for neutrino cross sections [15] and for polarized electron nucleon scattering [6] at low momentum transfers. In such extensions [17, 18] two neutral bosons occur with masses $M_1 \leqslant M_Z \leqslant M_2$, and the parameter v^2 is changed to

$$v^2 = (1-4\sin^2\theta_w)^2 + 16C,\ C \geqslant 0, \tag{18a}$$

where C is related to the gauge boson masses and couplings by

$$C = \gamma \cdot (M_1^2 - M_Z^2) \cdot (M_Z^2 - M_2^2)/(M_1 M_2)^2 \tag{18b}$$

γ has the value $\cos^4\theta_w$ in $G = \tilde{U}(1)$ (de Groot and Schildknecht [17]) and $\sin^4\theta_w$ in $G = SU(2)$ (Barger et al. [18]). Using $\sin^2\theta_w = 0.23$ the limit on v^2 is then essentially a limit on C. The PLUTO data yield

$$C < 0.06 \quad (95\%\ \text{c.l.}). \tag{19}$$

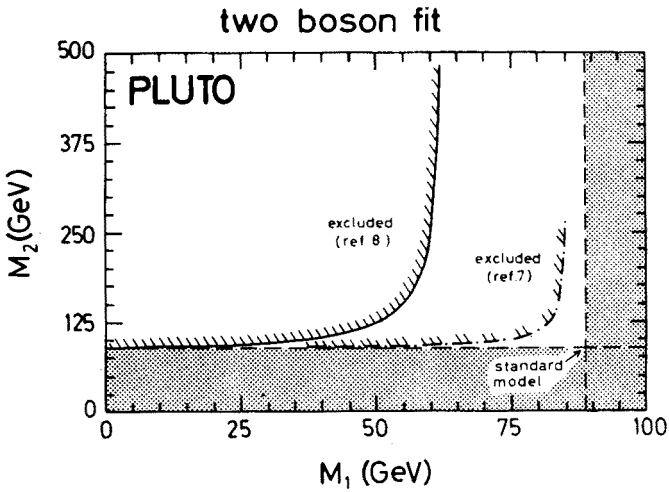

Fig. 10. 95% c.l. limits on the masses in the two neutral vector boson models of Refs. [17] (de Groot and Schildknecht) and [18] (Barger et al.). The dotted area is excluded by the models ($M_1 < M_Z < M_2$)

This imposes correlated bounds on M_1 and M_2 as shown in Fig. 10. We find that for the stronger coupling model ($\gamma = \cos^4\theta_w$, [17]) the mass of one of the two vector bosons can deviate from the Z_0 mass by at most 16%.

6. Summary and conclusion

In summary the PLUTO experiment has found:

(*i*) that QED is confirmed up to $s = 1000\ \text{GeV}^2$ and $q^2 = -850\ \text{GeV}^2$. The cutoff parameters correspond to distances of $1/\Lambda_+ \approx 2.10^{-16}$ cm down to which the validity

of QED has been probed. This is an improvement by a factor 3 as compared to pre-PETRA experiments;

(*ii*) no significant weak interaction effects at energies of $W \sim 30$ GeV, with an integrated luminosity of 2900 nb^{-1};

(*iii*) non-trivial limits on the strength of weak interactions in purely leptonic reactions.

Similar conclusions have been drawn from the JADE, MARK J, and TASSO experiments [14a, b, c]. A recent compilation of all PETRA experiments (as of August 1981) [14e] however yielded for the first time a significant asymmetry of

$$A = -(7.7 \pm 2.4)\% \tag{14a}$$

in disagreement with QED ($A = 0$, after radiative corrections), and in agreement with electroweak interference ($A = -7.8\%$) [3] at $\langle s \rangle = 1100$ GeV^2.

APPENDIX A

Formulae for QED modifications

A1. Cutoff parameterization

The modified Bhabha cross section, with $q^2 = -s \sin^2 \frac{\theta}{2}$, and $q'^2 = -s \cos^2 \frac{\theta}{2}$, reads

$$\frac{d\sigma}{d\Omega} = \frac{\alpha^2}{2s} \left\{ \frac{q'^4 + s^2}{q^4} |F_S(q^2)|^2 + \frac{2q'^4}{q^2 s} \mathrm{Re}(F_S F^*_T) + \frac{q'^4 + q^4}{s^2} |F_T(s)|^2 \right\} \tag{A.1a}$$

$$= \frac{d\sigma_{\mathrm{QED}}}{d\Omega} (1 + \delta_A(s, \theta)) \tag{A.1b}$$

with $\delta_{A\pm}(s, \theta) = \dfrac{3s}{A_\pm^2} \dfrac{1 - \cos^2 \theta}{3 + \cos^2 \theta} + O(s^2/A^4)$.

For $A = 100$ GeV, $\sqrt{s} = 31$ GeV: $\delta_A \sim 10\%$ at 90° and zero at 0°. The $\mu^+\mu^-$ and $\tau^+\tau^-$ cross sections which have contributions from time-like photons only, for $\sqrt{s} \gg m_\tau, m_\mu$ read:

$$\frac{d\sigma}{d\Omega} = \frac{\alpha^2}{4s} (1 + \cos^2 \theta) |F_T(s)|^2 \tag{A.2a}$$

$$= \frac{d\sigma_{\mathrm{QED}}}{d\Omega} (1 + \delta_A(s)) \tag{A.2b}$$

with $\delta_{A\pm}(s) = \pm \dfrac{2s}{A_\pm^2} + O(s^2/A^4)$.

In this case δ_A is independent of θ; for $A = 100$ GeV, $\sqrt{s} = 31$ GeV: $\delta_A \sim 20\%$. For $ee \to \gamma\gamma$ two different modifications have been considered in the literature:

(a) Propagator and vertex modifications

Here it can be shown [4e, 4g, 15] that all contributions of the order (q^2/Λ^2) cancel and that the amplitude modification can be parameterized by form factors:

$$F(q^4) = 1 \pm \frac{q^4}{\Lambda_\pm^4}. \tag{A.3}$$

Hence

$$\frac{d\sigma}{d\Omega} = \frac{\alpha^2}{2s}\left\{\frac{q'^2}{q^2}|F(q^4)|^2 + \frac{q^2}{q'^2}|F(q'^4)|^2\right\} \tag{A.4a}$$

$$= \frac{d\sigma_{\text{QED}}}{d\Omega}(1+\delta_\Lambda(s,\theta)) \tag{A.4b}$$

with $\delta_{\Lambda_\pm}(s,\theta) = \pm \frac{s^2}{2\Lambda_\pm^4}\frac{\sin^4\theta}{1+\cos^2\theta} + O(s^4/\Lambda^8)$.

(b) Heavy electron (E*) exchange

Here the interference of the normal (e) and heavy electron (E*) is considered

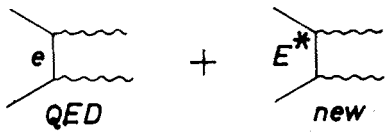

Current conservation allows only for a magnetic moment coupling between e, E* and γ.

A quantitative calculation [4h] yields

$$\delta_\Lambda = \frac{s^2}{2\Lambda^4}\cdot\sin^2\theta + O(s^4/\Lambda^8). \tag{A.4c}$$

The parameter Λ is related to the mass M_E and to the coupling constant λ of the excited electron by $\Lambda^2 = M_E^2/\lambda^2$.

In both cases (a) and (b) the modifications are maximum at $\theta = 90°$. They are numerically smaller than in the case of Bhabha scattering of lepton pair production (e.g. $\Lambda = 100$ GeV, $\sqrt{s} = 31$ GeV: $\delta \sim 0.4\%$ at $\theta = 90°$) which is reflected in correspondingly lower experimental limits on Λ.

A more detailed presentation can be found in Refs [4h, 19].

A2. Electroweak cross sections

From the standard 1st order Hamiltonian of the electroweak neutral current one can derive [20] the following differential cross sections (neglecting terms of the order m_e^2/s).

(a) $e^+e^- \to e^+e^-$:

$$\frac{4s}{\alpha^2}\frac{d\sigma}{d\Omega} = \left\{\frac{3+x^2}{1-x}\right\}^2 + 2\frac{3+x^2}{(1-x)^2}\{(3+x)Q - x(1-x)R\}v^2$$

$$-\frac{2}{1-x}\{(7+4x+x^2)Q+(1+3x^2)R\}a^2+\tfrac{1}{2}\left\{\frac{16}{(1-x)^2}Q^2+(1-x)^2R^2\right\}(v^2-a^2)^2$$

$$+\tfrac{1}{2}(1+x)^2\left\{\left(\frac{2}{1-x}Q-R\right)\right\}^2(v^4+6v^2a^2+a^4), \tag{A.5}$$

with $x = \cos\theta$, θ being the polar angle with respect to the beam axis

$$Q = gM_Z^2\frac{q^2}{q^2-M_Z^2} \to -gq^2 = \delta\cdot s\,\tfrac{1}{2}(1-x) \quad (M_Z^2 \gg |q^2|),$$

$$R = gM_Z^2\frac{s}{s-M_Z^2} \to -gs \quad (M_Z^2 \gg s),$$

$$g = \frac{G_F}{8\sqrt{2}\,\pi a} = 4.49\cdot 10^{-5}\,(\mathrm{GeV}^{-2}),$$

$\alpha = 1/137$, fine structure constant, G_F = Fermi coupling constant, M_Z = mass of the Z^0 boson, $q^2 = -\frac{s}{2}(1-\cos\theta) = -\frac{s}{2}(1-x)$.

The coupling strengths of the vector and the axial weak current are expressed by v and a. Their normalization is such that $a^2 = 1$, $v^2 = (1-4\sin^2\theta_w)^2$ in the standard electroweak model [3].

(b) $e^+e^- \to \mu^+\mu^-$:

$$\frac{4s}{\alpha^2}\frac{d\sigma}{d\Omega} = (1+x^2)\{1+2v^2R+(v^2+a^2)^2R^2\}+4x\{a^2R+2v^2a^2R^2\} \tag{A.6a}$$

$$\sigma = \frac{4\pi\alpha^2}{3s}\{1+2v^2R+(v^2+a^2)^2R^2\}. \tag{A.6b}$$

In equations (A.5) and (A.6) the terms independent of Q and R correspond to the pure QED contributions, the terms linear in Q, R describe the electroweak interference and the terms in Q^2, R^2 are pure weak contributions.

The interference term in $ee \to \mu\mu$ produces a forward-backward asymmetry A, which is sensitive to a^2. If μ pairs are measured at production angles $|\cos\theta| < x_1$ Eq. (A.6) yields

$$A(x_1) = \frac{6x_1}{3+x_1^2}\,\frac{a^2R(1-2v^2R)}{1+2v^2R+(v^2+a^2)^2R^2}. \tag{A.7}$$

APPENDIX B

Data analysis in QED reactions

In this appendix we give details on the event selection — at the trigger level and in the off-line analysis — for the four QED reactions (1)-(4), and also on how the main background sources were removed. A few QED event pictures are shown in Fig. 11.

B1. $e^+e^- \to e^+e^-$

At runs below 22 GeV, Bhabha events [13a, 21] were triggered by a coincidence of two opposite shower counters if more than 1.2 GeV was observed in each, or by a trigger sensitive to more than 3 GeV in the full shower counter. For runs at 27–31 GeV these threshold values were doubled. The efficiency of these triggers for Bhabha events was as high as $99.9 \pm 0.1\%$. This could be measured by an independent track trigger for Bhabha events.

After shower reconstruction events with (at least) 2 showers with energies $E_{SH} > E_B/3$ each were accepted for the further analysis. The tracks were reconstructed and matched with the shower position. Events with no tracks pointing to the showers or with more than 4 tracks from a common vertex were rejected. Allowing for more than 2 tracks is necessary because some events start showering in the track detector. The sample now consisted of 2-prongs if both showers were associated with tracks, and of a few ($\sim 4\%$) 1-prongs. Within the acceptance (Table I) the efficiency for recognizing an $e^+e^- \to e^+e^-$ event was determined to be $99.3 \pm 0.4\%$. The resolution of the scattering angle is $\sigma(\cos\theta) = 0.01$, independent of $\cos\theta$.

The main *background* source was the reaction $e^+e^- \to \gamma\gamma$, where one or both γ's started showering in the track detector. The 1-prong sample was cleared from this background in a visual scan. From the analysis of the reaction $ee \to \gamma\gamma$, and the number of $e^+e^- \to \gamma\gamma$ with 1γ converted, the contamination of the 2-prong Bhabha sample from this source was calculated to be $0.3 \pm 0.03\%$. All other backgrounds (beam, gas, cosmic rays, $ee \to \tau\tau$, $ee \to ee + ee$, $ee + \mu\mu$) were less than 1% together.

The reliability of charge identification could be checked in the 2-prong Bhabha sample which contained a small fraction ($\sim 5\%$) of events with two same charge tracks. From this number we have determined the number of events with two prong curvature tracks at each energy and $\cos\theta$ interval for corrections. The same charge 2-prong events were divided according to the ratio of forward/backward scatters. Corrections of the few 1-prong Bhabhas could be neglected. In addition all backward scatters were checked in a visual scan. The separation of forward-backward Bhabha scattering does not affect the determination of the cut-off parameters Λ (Eq. A.1b), but is useful for the analysis of electroweak effects.

B2. $e^+e^- \to \gamma\gamma$

Trigger and event preselection were similar as for Bhabha events (Section B.1) with slightly different acceptance and acollinearity cuts (see Table I) and by requiring $E_{SH} \geq 1/4\, E_B$ [13b, 21]. In this sample $\gamma\gamma$ final states were separated from ee, eeγ and hadronic final states mainly by rejecting events where

(a) both clusters were associated with tracks,
(b) more than 5 tracks were observed in the track detector,
(c) the angle between any two reconstructed tracks exceeded 50°.

The $\gamma\gamma$ candidates were then scanned visually. Among the events with no tracks in the track detector ($\sim 60\%$ of the total sample) practically no background was found, in agreement with a Monte Carlo study. The remaining events could be separated into

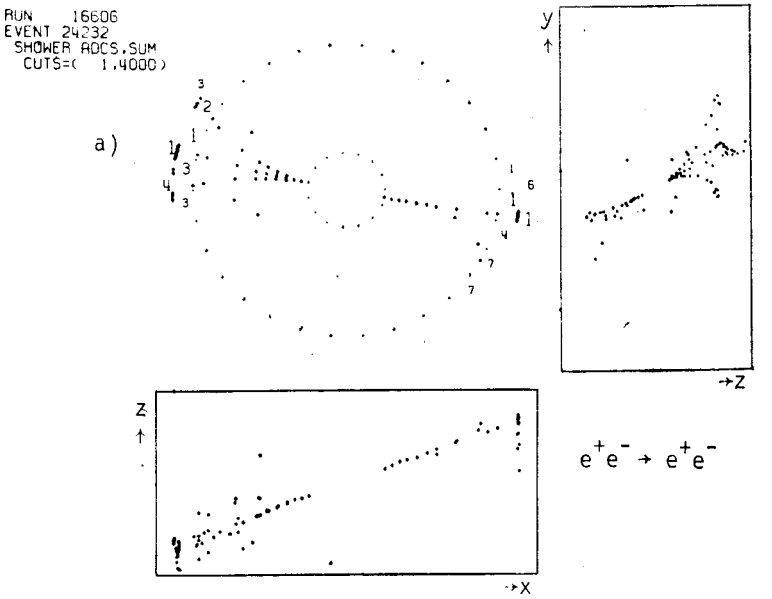
RUN 16606
EVENT 24232
SHOWER ADCS.SUM
CUTS=(1.4000)
a)
y
z
x
$e^+e^- \rightarrow e^+e^-$

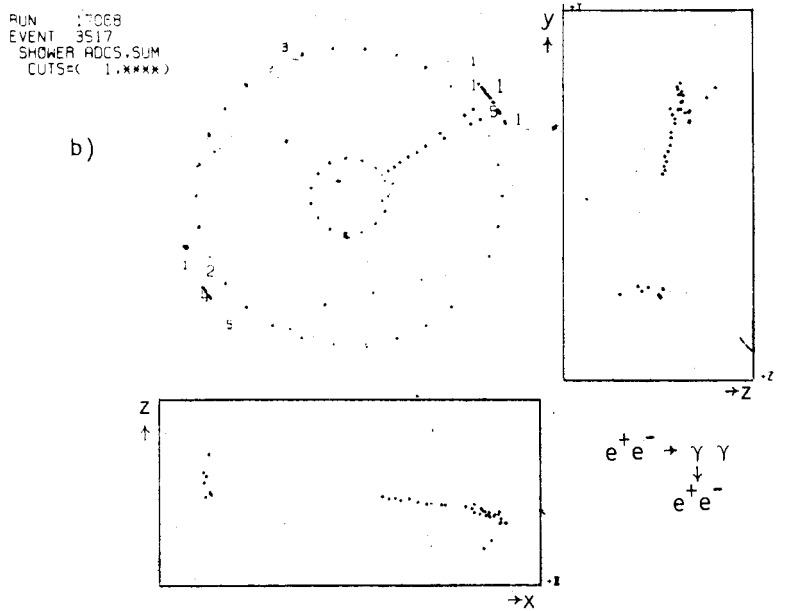
EVENT 3517
SHOWER ADCS.SUM
CUTS=(1.****)
b)
y
z
x
$e^+e^- \rightarrow \gamma\gamma$
e^+e^-

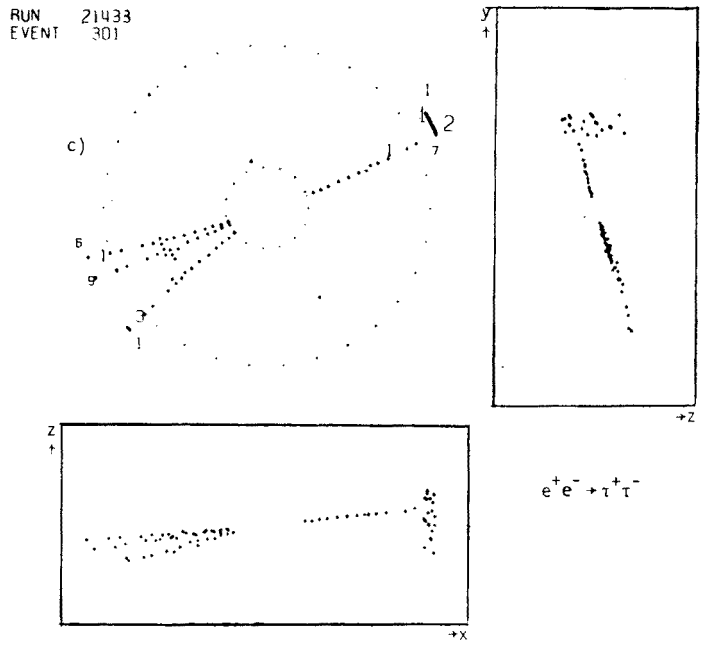

Fig. 11. Event pictures in PLUTO; (a) for $e^+e^- \to e^+e^-$ with pair production in the beam pipe by one outgoing track, (b) for $e^+e^- \to \gamma\gamma$ with one photon conversion in the beam pipe, and (c) for $e^+e^- \to \tau^+\tau^-$ in a 4-prong final state. The pictures show a view along the beam (circular graph), and two orthogonal projections perpendicular to the beam

(*i*) $\gamma\gamma$ final states with one converted photon ($\sim$30% of the total $\gamma\gamma$ rate), and (*ii*) Bhabha scatters with one shower in the track detector without reconstructed tracks, eeγ final states and a small number of hadronic final states. The events from (*ii*) were rejected.

A total of 1034 events was accepted, with an estimated background of (1 ± 1)%. Losses came from the selection cuts (5.5 ± 1.1%) and incorrectly analysed shower patterns (1.3%), leading to an overall efficiency of 93 ± 2%.

B3. $ee \to \mu\mu$

The events were triggered by a track trigger sensitive to two coplanar tracks. In selecting this final state [13d, 22] the main problem is the rejection of cosmic ray background. All other backgrounds from $ee \to$ hadrons, $ee \to ee$, $ee \to ee + \mu\mu$ are negligible, or small (2% from $ee \to \tau\tau$) in 2 prong events which passed the following cuts:

(*i*) two tracks with $|\cos\theta| < 0.75$,

(*ii*) collinear within 10°,

(*iii*) track momenta $p > 0.5\ (0.67) \cdot E_B$ for $E_B > 10$ (<10) GeV; (for collinear tracks we find a momentum resolution of $\sigma_p \leqslant 0.01\ p^2$),

(*iv*) distance of tracks to the interaction point small: $\Delta r(x, y) < 1.5$ mm, $\Delta z < 40$ mm,

(*v*) total energy in shower counters $E_{SH} < 1$ GeV,

(*vi*) time difference of < 20 (60) nsec between event time from barrel (end cap) and beam crossing.

After these cuts the cosmic ray background in the end cap region was 40% of the μ pair signal and was subtracted, using a side band in event time. In the barrel region, ($|\cos\theta| < 0.6$) a time of flight separation was possible. Fig. 12 shows the time difference of the 2 back-to back tracks normalized to incidence perpendicular to the beam. Cosmic rays and μ-pairs are clearly separated by a cut at 2 nsec, leaving a cosmic ray background

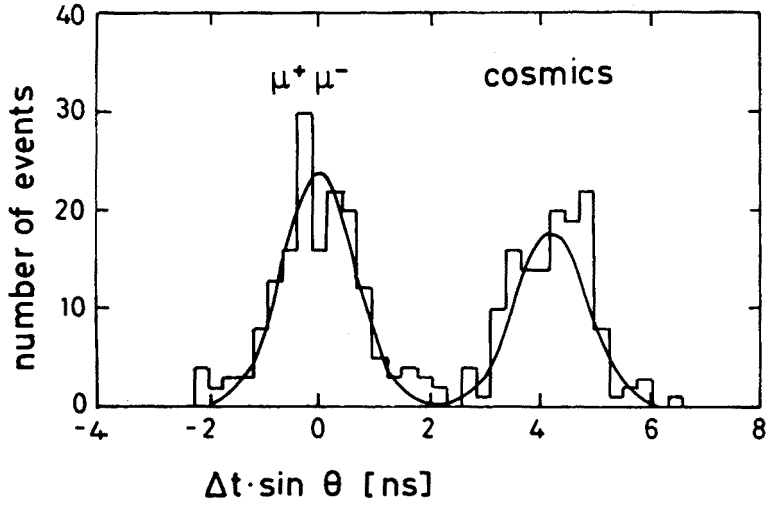

Fig. 12. TOF difference for μ pairs and cosmics

of less than 1.4%. After background subtractions we obtain 228 μ-pair events. The trigger efficiency is 98%, and the event selection cuts are associated with losses of 1.5%.

At the present level of statistics, errors in the asymmetry from uncertainties in charge sign identification are completely negligible. For $W = 30$ GeV, the sagitta in a collinear 2-track fit is different from zero by ~7 standard deviations.

B4. $ee \to \tau\tau$

This reaction is new in the context of testing QED. In principle it provides the same information as $ee \to \mu\mu$, but in practice there are several drawbacks from the fact that τ's are not observed before they decay: cross sections have to be determined from decay channels using branching ratios which are known with a limited accuracy, and the production angle of τ's cannot exactly be reconstructed from the decay products.

On the other hand, at energies $W \gg 2 \cdot m_\tau$ the signature of τ pair events becomes much clearer than at the low energies ($E_B \sim 2$ GeV), where the τ lepton was discovered. The most distinctive features of τ pair events at PETRA energies are a low multiplicity (2-, 4- and a few 6-prongs, as compared to $\langle n_{CH} \rangle \sim 10$ for hadronic annihilation, and two almost collinear sets of decay products contained in very small solid angles (see Figs 11c and 13). We have used final states in which at least one τ lepton decays into only one charged particle (e, μ, π) plus neutrals [13d, 23]. This way we accept ~90% of all decay modes [16]. The accepted events then consist of 2 prongs (~50% of all) and 4 prongs (~40%) which require different additional cuts for background rejection.

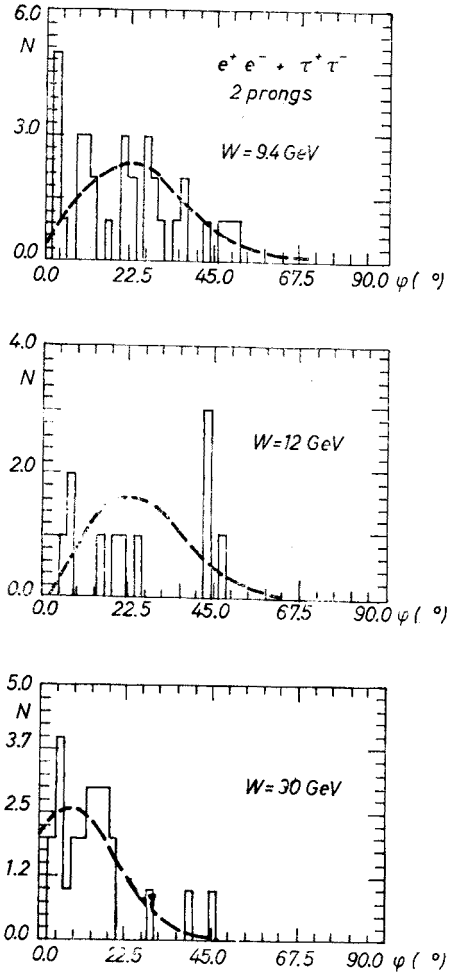

Fig. 13. Acollinearity angle distribution in $e^+e^- \to \tau^+\tau^-$ 2 prong events, at $W = 9.4$, 12, and 30 GeV

The main background problem in the 2-prong events is due to ee → ee, μμ, and to cosmic rays, and γγ reactions. 2-prong τ events were selected by applying the following selection criteria.

(1) 2 oppositely charged tracks, originating from the interaction point,
(2) one momentum $p > 0.8$ GeV/c, the other $p > 0.5$ GeV/c (mainly against beam gas),
(3) production angle of each track $|\cos\dot{\theta}| < 0.6$; (to have time of flight rejection of cosmic rays),
(4) no collinear fit possible (against μ-pairs and remaining cosmics),
(5) missing mass $> 0.5\, E_{\text{beam}}$ (against μμγ, eeγ),
(6) an acoplanarity angle $\alpha > 18°$, if both tracks are associated with showers of energies $E > 0.25\, E_{\text{beam}}$ (against radiative Bhabhas, see also Fig. 5 for α distribution of Bhabha events),

(7) 2-prong effective mass $M > 2$ (3) GeV at $E_{CM} \leqslant 13$ ($\geqslant 17$) GeV, and net momentum transverse to the beam > 0.5 GeV/c (against $\gamma\gamma$ events).

According to a simulation of reaction (4) 17% of all 2-prong events passed these criteria [23]. 4-prong events are of the following type

$$\begin{array}{ccc} ee \to \tau & & \tau \\ \downarrow & & \downarrow \\ 1 \text{ prong} & & 3 \text{ prong} \\ +\text{neutrals} & & +\text{neutrals} \end{array}$$

with the 1- and 3-prong parts almost back to back. The main background in this topology is from $\gamma\gamma$ reactions and from degraded Bhabha events. To select τ events we required

(1) $\leqslant 6$ observed charged tracks (to allow for one $\gamma \to e^+e^-$ conversion) with no charge excess,

(2) all tracks with $|\cos\theta| < 0.75$,

(3) at least 1 track with $p > 0.4$ (0.5) GeV at $E_{Cm} \leqslant 13$ ($\geqslant 17$) GeV, and with no other tracks within $\Delta\phi = \pm 90°$ ("1-prong"),

(4) the 3-prong mass consistent with τ decay,

(5) cut (7) of 2-prongs with appropriate modifications to reject $\gamma\gamma$ events (in particular $\gamma\gamma \to \tau\tau$; two clear examples of such events have been observed).

20% of all 4-prongs passed these criteria.

After these cuts we find 73 2-prong events and 78 4-prong events. The remaining background, (3 2-prong and 9 4-prong events), due to $\gamma\gamma$ processes and multihadron events, was estimated by Monte Carlo simulations of these processes.

The efficiency of triggering and event selection, as well as the radiative corrections were determined from a Monte Carlo simulation which includes radiation in the initial state and τ production and decay into the various channels in the detector. We have checked [23] that the relative ratios of various subchannels with identified particles like e, μ, π, ϱ, and the 2- and 4-prong ratio are consistent with the τ decay branching ratios [16].

Editorial note. This article was proofread by the editors only, not by the author.

REFERENCES

[1] A recent review of experimental QED tests can be found in: J. J. Sakurai, Conference on High Energy e^+e^- Interactions, (Vanderbilt, 1980), AIP Conference Proceedings No. 62 (1980), and preprint UCLA/80/TEP/14.

[2] R. P. Feynman, *Phys. Rev.* **76**, 769 (1949).

[3] S. L. Glashow, *Nucl. Phys.* **22**, 579 (1961); S. Weinberg, *Phys. Rev. Lett.* **19**, 1264 (1967); A. Salam, *Elementary Particle Theory*, ed. N. Svartholm, Almquist and Wiksell, Stockholm 1968, p. 367.

[4] (a) F. Boop, *Ann. Phys.* (Germany) **42**, 573 (1942); R. P. Feynman, *Phys. Rev.* **74**, 939 (1948).
(b) H. Salecker, *Z. Naturforsch.* **8a**, 16 (1953); and **10a**, 349 (1955).
(c) S. D. Drell, *Ann. Phys.* (USA) **4**, 75 (1958).
(d) F. E. Low, *Phys. Rev. Lett.* **14**, 238 (1965).
(e) J. A. McClure, S. D. Drell, *Nuovo Cimento* **37**, 1638 (1965).

(f) R. Gatto, Proceedings of the Intern. Symposium on Electron and Photon Interactions at High Energies, Vol. 1, p. 106, Deutsche Physikalische Gesellschaft 1965, Hamburg 1965.
(g) N. M. Kroll, *Novo Cimento* **45**, 65 (1966).
(h) A. Litke, Harvard University, Ph. D. Thesis (1970), unpublished.
(i) K. Ringhofer, H. Salecker, Contribution to the 1975 Internat. Symposium on Lepton and Photon Interactions at High Energies, Stanford University, unpublished, and Contribution to the 19th International Conference on High Energy Physics, Tokyo 1978, unpublished.
(j) M. Capdequi Peyranère et al., *Nucl. Phys.* **B149**, 243 (1979).

[5] For $\Gamma(T \to ee)$: PLUTO Collaboration, C. H. Berger et al., *Z. Phys.* **C8**, 101 (1981), for $\Gamma(v \to ee)$, $v = \varrho, \omega, \phi$, J/ψ and ψ' see Ref. [16].

[6] C. Y. Prescott et al., *Phys. Lett.* **77B**, 347 (1978); **84B**, 524 (1979).

[7] L. M. Barkov, M. S. Zolatosyov, *Phys. Lett.* **85B**, 308 (1979).

[8] J. E. Augustin et al., *Phys. Rev. Lett.* **34**, 233 (1975); L. H. O'Neil et al., *Phys. Rev. Lett.* **37**, 395 (1976).

[9] (a) G. Bonneau, F. Martin, *Nucl. Phys.* **B27**, 381 (1971).
(b) F. A. Berends, K. J. F. Gaemers, R. Gastmans, *Nucl. Phys.* **B57**, 381 (1973); **B63**, 381 (1973); **B68**, 541 (1974); F. A. Berends, G. J. Komen, *Phys. Lett.* **63B**, 432 (1976); F. A. Berends, R. Kleiss, DESY 80/66.

[10] F. A. Berends, R. Gastman, *Nucl. Phys.* **B61**, 414 (1973).

[11] Weak interaction effects in reaction (2) have been discussed by many authors. Some of the earliest papers are: N. Cabibbo, R. Gatto, *Phys. Rev.* **124**, 1577 (1961); T. Kinoshita et al., *Phys. Rev.* **D2**, 910 (1970); J. Godine, A. Hankey, *Phys. Rev.* **D6**, 3301 (1972); R. Budny, *Phys. Lett.* **45**, 340 (1973); For reviews see, e.g. L. Wolfenstein, *AIP Proceedings* **23**, 84 (1974); J. J. Sakurai, *AIP Proceedings* **51**, 138 (1979).

[12] (a) J. Takahashi, *Nuovo Cimento* **6**, 370 (1957).
(b) F. E. Low, *Phys. Rev.* **110**, 974 (1958).

[13] (a) PLUTO Collaboration, Ch. Berger et al., *Z. Phys.* **C4**, 269 (1980).
(b) PLUTO Collaboration, Ch. Berger et al., *Phys. Lett.* **94B**, 87 (1980).
(c) PLUTO Collaboration, Ch. Berger et al., *Z. Phys.* **C7**, 289 (1981).
(d) PLUTO Collaboration, Ch. Berger et al., submitted to *Phys. Lett.* B, DESY 81/001.

[14] (a) JADE Collaboration, W. Bartel et al., *Phys. Lett.* **92B**, 206 (1980); W. Bartel et al., Preprint DESY 80/123, to be published in *Phys. Lett.* B.
(b) MARK J Collaboration, D. P. Barber et al., *Phys. Rev. Lett.* **42**, 1110 (1979); *Phys. Rev. Lett.* **43**, 1915 (1979), MARK J Collaboration, *Phys. Rep.* **63**, 337 (1980).
(c) TASSO Collaboration, R. Brandelik et al., *Phys. Lett.* **94B**, 259 (1980); *Phys. Lett.* **92B**, 199 (1980).
(d) For a summary as of June 1981 see: P. Dittmann, V. Hepp, to be published in *Z. Phys.* C, and DESY 81/030.
(e) J. G. Branson, invited talk at the 1981 International Symposium on Lepton and Photon Interactions at High Energies, Bonn 1981.

[15] e.g. K. Winter, Proc. of the International Symposium on Lepton and Photon Interactions at High Energies, Fermilab 258/1979.

[16] Particle Data Group, *Rev. Mod. Phys.* **52** (1980).

[17] E. H. de Groot, D. Schildknecht, *Phys. Lett.* **90B**, 427 (1980); E. H. de Groot, D. Schildknecht, Univ. Bielefeld Report, BI-TP 80/08.

[18] V. Baeger et al., *Phys. Rev. Lett.* **44**, 1169 (1980).

[19] V. Hepp, *Test of Quantum Electrodynamics at high momentum transfers*, talk given at the Symposium on *Stand und Ziele der QED*, Mainz, May 9-10, 1980, submitted for publication in *Lecture Notes on Physics*, Springer Verlag.

[20] R. Budny, *Phys. Lett.* **55B**, 227 (1975); *Phys. Lett.* **45B**, 340 (1973).

[21] B. Koppitz, Ph. D. Thesis, Hamburg 1980 and int. rep. DESY-PLUTO 80/05.

[22] W. Luhrsen, Ph. D. Thesis, Hamburg, in preparation.
[23] O. Meyer, Ph. D. Thesis, Wuppertal 1980, internal report DESY PLUTO — 81/01.
[24] A. A. Sokolov, J. M. Ternov, *Sov. Phys. Dokl.* **8**, 1203 (1964). For a recent review see J. D. Jackson, *Rev. Mod. Phys.* **48**, 417 (1976).